


Handbook
for
Generic Photonic IC Design

Editors: Meint Smit and Xaveer Leijtens

4-4-2026

 *Handbook for generic photonic IC design*, by the *Photonic Integration group*, Technische Universiteit Eindhoven, is licensed under a Creative Commons “Attribution-NonCommercial-NoDerivatives 4.0 International” license.

We traced the ownership of all figures used as far as we could. However, if you are a copyright owner and believe we used your work without permission, please contact us at coordinator@jeppix.eu.

Chapter 21

Tapers and Spot-Size Converters

MEINT SMIT

Tapers and Spot-Size Converters or Mode-Field Adapters are different names of a component for smooth adaption of the size and shape of the modes between different waveguides or between a waveguide and a lensed or cleaved fiber, in order to reduce the coupling losses. It can be conceived as a concatenation of a large number of short straight waveguide sections with increasing or decreasing width, and indeed some modeling tools calculate its properties in this way. We have, therefore, placed it in part III: Composite Building Blocks.

taper
spot-size converter
mode-field adapter

In this chapter the tapers and Spot-Size converters used in the JePPIX foundries will be discussed. In Section 21.1 we describe two-dimensional waveguide tapers. They expand or compress the waveguide mode in one direction, the lateral direction. In the vertical direction they do not change the mode width, which is typically in the order of 0.5 μm . For low loss coupling between a waveguide and a lensed or cleaved fibre the waveguide mode needs to be expanded in two directions. This is described in Section 21.2. In Subsections 21.2.1 and 21.2.2 the spot-size converters of the HHI and SMART Photonics foundries are briefly discussed.

21.1 Waveguide tapers

The simplest way for low-loss connection of two waveguides with different widths is by using a linear taper. If the taper angle is sufficiently small the mode profile will adapt itself smoothly to the changing waveguide width without mode conversion or radiation loss. Such a taper is called an adiabatic taper. Figure 21.1 shows an example of an adiabatic taper and a taper which has been designed too short and shows significant mode conversion.

linear taper
adiabatic taper

To keep the length as small as possible a trade-off has to be made between taper length and insertion loss. An optimal value should be calculated with a numerical simulation tool. A first estimate, which can serve as starting value in the numerical analysis, can be made with ray theory (see Chapter 2 Section 2.4.1. It is illustrated in figure 21.2.

Support from Limeng Zhang for checking the text and the calculations, and generating some of the graphs, is gratefully acknowledged.

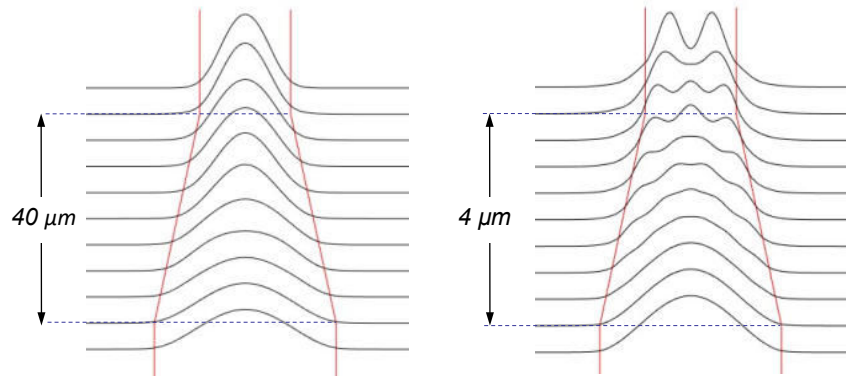


Figure 21.1: Adiabatic taper and taper with mode conversion

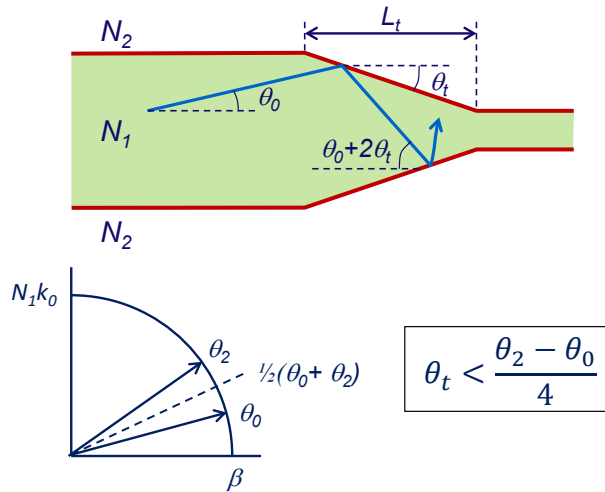


Figure 21.2: Conversion to the 2nd-order mode at a tapered waveguide edge.

In the taper region the rays with propagation angles $\pm\theta_0$, which represent the fundamental mode, will get angles $\pm(\theta_0 + 2\theta_t)$ after reflection. If these angles come close to the propagation angles $\pm\theta_2$ of the second-order mode¹ strong conversion to the second order mode will occur, as can be observed in Figure 21.1 (right). In designing the taper we have to stay away from this angle and a rule of thumb is to design the taper such that after reflection the propagation angle is halfway the propagation angles of the fundamental and the second-order mode: $\theta_0 + 2\theta_t = \frac{1}{2}(\theta_0 + \theta_2)$ or

$$\theta_t = \frac{1}{4}(\theta_2 - \theta_0) \quad (21.1)$$

For a linear taper the design should be based on the propagation angles at the wide side of the taper, here the propagation angles and their difference are the smallest and, consequently, the taper angle should also be small. This can also be understood by considering the diffraction of the mode shown in Figure 21.1 (left) when propagating from the top to the bottom. When the beam comes out of the narrow waveguide and

¹In a symmetric taper conversion of the symmetric fundamental mode to the anti-symmetric first-order mode cannot occur.

Problem: The first part of a Y-junction is usually a linear taper to twice the waveguide width (taper ratio 2), from whereon the waveguides start to separate. Estimate the length of such a taper, designed according to Equation 21.1, for the standard shallow waveguide as described in Problem 2.18.

Solution: The taper length follows from the formula $L \tan \theta_t = \{w(L) - w(0)\} / 2 = \Delta w / 2$ as $L = \frac{1}{2} \Delta w / \tan \theta_t$. If $w(L) = 2w(0)$ then $\Delta w = w(0) = w$. We will do the calculation with the Effective Index Method (see Section 2.5.1). In this approach a numerical 2D mode solver is used for first calculating the effective indices in the vertical direction and subsequently calculating the modes in the lateral direction. For the vertical stack in and beside the ridge we found (see Problem 2.14) $N_{eff} = 3.27$ and 3.20 , respectively for the TE_0 -mode. With these values we find for the lateral TM_0 -mode $N_{eff} = 3.2659$ and for the lateral TM_2 -mode $N_{eff} = 3.2339$, using a numerical slab mode solver. The propagation angle for the fundamental lateral mode is $\theta_0 = \arccos(3.2659/3.27) = 2.9^\circ$. For the second order mode $\theta_2 = 8.5^\circ$. For the maximum taper angle we find $\theta_t = (\theta_2 - \theta_0)/4 = (8.5 - 2.9)/4 = 1.4^\circ$. With this taper angle the length of the taper is $L_t = \frac{1}{2} w / \tan \theta_t \approx 40 \mu\text{m}$. This taper angle can be used as starting point for a numerical 3D-computation.

Problem: Do the same for a deep-etched waveguide with $w = 1.5 \mu\text{m}$. Apply the Effective Index Method with $N_0 = N_2 = 1$ in the deep etched regions beside the waveguide.

Solution: For the deep-etched waveguide we find $N_{eff} = 3.2599$ and 3.1778 for the effective indices of the lateral TM_0 and TM_2 -mode, respectively. The corresponding propagation angles are $\theta_0 = \arccos(3.2599/3.27) = 4.5^\circ$ and $\theta_2 = \arccos(3.1778/3.27) = 13.6^\circ$. For the maximum taper angle we thus find $\theta_t = (13.6 - 4.5)/4 = 2.3^\circ$. With this angle $L_t = \frac{1}{2} 1.5 / \tan 2.3 \approx 19 \mu\text{m}$.

Problem 21.1: Taper design.

enters the taper section, the rate of widening is restricted by diffraction. When the taper angle is larger than the divergence of the beam due to diffraction, it will not follow the taper. See Chapter 2 Section 2.2.5. When the beam-width is narrow, the divergence is large, and hence the taper angle can be large. When the beam becomes wider, the divergence and hence the maximum taper angle decrease.

Parabolic taper Figure 21.3 shows how the difference $\Delta\theta_{02}$ between the fundamental and the second-order mode increases along the taper when the waveguide width decreases. For an optimal taper design we have to adapt the local taper angle to $\Delta\theta_{02}$, so that it is smallest for the largest width and increases with decreasing width. In this way we get a so-called parabolic taper as shown in the figure.

parabolic taper

The reduction of the taper length for a parabolic taper is modest: for a taper ratio of 2 the length reduces with 25%, for a taper ratio of 4 with 37%, see figure 21.4. However, this size reduction essentially comes for free.

Insertion Loss Figure 21.5 shows the insertion loss of a linear taper with a taper ratio 2 as a function of the taper length and angle, both for shallow and deep standard waveguides (with 2 and $1.5 \mu\text{m}$ waveguide width, respectively). Passive tapers are reciprocal;

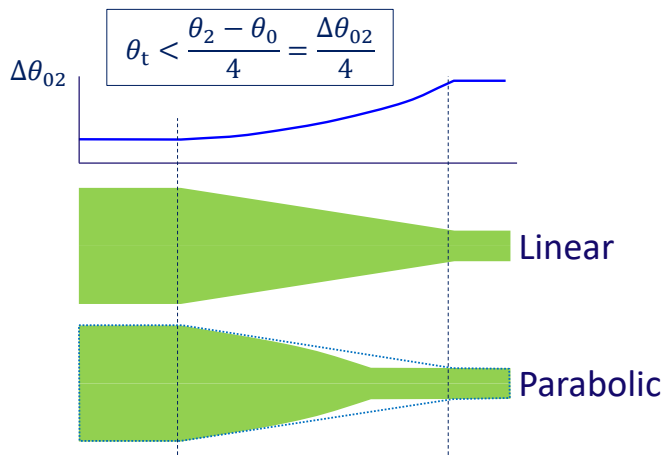


Figure 21.3: Taper types.

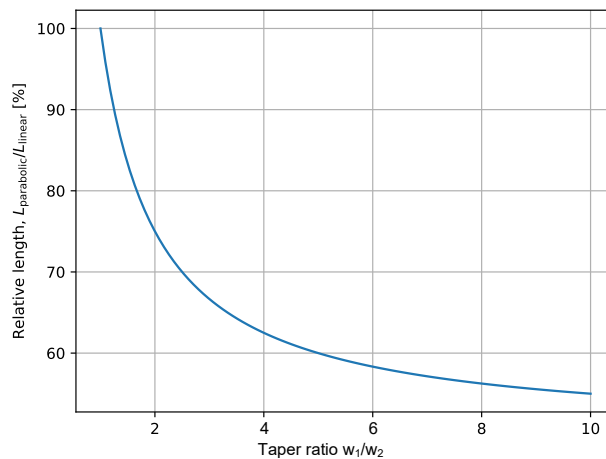


Figure 21.4: The relative length of a parabolic taper versus a linear taper as a function of the taper ratio w_1/w_2 .

Problem: Calculate the shape $w(z)$ of a taper according to Formula 21.1, starting from a waveguide with width $w(0)$.

Solution: For wider waveguides the difference $\theta_2 - \theta_0$ decreases inversely proportional to the waveguide width. Because the taper angle equals dw/dz , dw/dz is inversely proportional to $w(z)$ and, consequently, the taper shape is parabolic: $w(z) = w(0)\sqrt{(z + z_0)/z_0}$ in which $w(0)$ is the taper width at $z = 0$. The derivative $dw/dz = \{w(0)/(2\sqrt{(z + z_0)/z_0})\} \cdot \frac{1}{z_0}$ equals the taper angle according to Formula 21.1: $dw/dz = \frac{1}{4}\Delta\theta_{02}$. From this we find $z_0 = 2w(0)/\Delta\theta_{02}(0)$ in which $\Delta\theta_{02}(0)$ is the value of $\Delta\theta_{02}$ at $z = 0$.

Problem 21.2: Taper design.

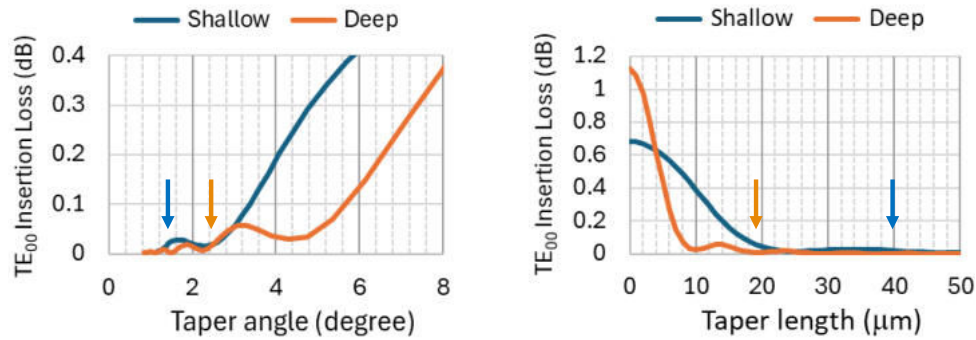


Figure 21.5: Insertion loss of linear tapers with varying length, for shallow and deep etched waveguides.

the transmission of a mode from narrow to wide equals the transmission from wide to narrow. From the upper figure we see that for taper angles below 3° the insertion loss is well below 0.1 dB. The arrows indicate the angles calculated from Eq. 21.1 and the corresponding taper lengths. We see that the formula is very conservative. Practical designs can be shorter by almost a factor of 2 without introducing significant loss. This could be expected because the formula is based on the mode conversion in the widest part of the taper. In the narrower part the angular distance between the modes is larger and, consequently, the mode conversion will be smaller.

From the Figure we see that the deep etched taper can be designed shorter than the shallow etched one, which is to be expected because the deep etched waveguide is narrower and has a higher lateral confinement. As a result it can be tapered faster without significant mode conversion.

From the figure we see that the shallow and deep etched taper have a minimum insertion loss around 25 and 10 μm taper length, respectively. For larger length the loss increases again slightly up to a maximum around 35 and 14 μm taper length, respectively, after which it decreases again.

This effect is due to excitation of the 2nd-order mode, which means that the taper is not adiabatic. Because both modes have different propagation constants, their interference is dependent on the length of the taper. Power coupled to the second order mode at the beginning of the taper can interfere constructively or destructively with power converted further down the taper, dependent on the length of the taper. Obviously, for 25 and 10 μm taper length they interfere destructively, whereas for 35 and 14 μm they interfere constructively, analogous to what happens in MMI-couplers. We can use this interference to reduce the length of the taper. However, such a non-adiabatic taper, which is designed for destructive interference, is less tolerant on waveguide geometry and polarisation than an adiabatic taper. It should be noted that even in the constructive interference point the insertion loss is far below 0.1 dB, so the penalty of a shorter design is small. But if modal purity, fabrication tolerance or polarisation independence are important we should design it longer.

21.2 Spot-size converters

Planar waveguide tapers, as described in the previous section, offer an easy means of adapting the width of a waveguide mode to the requirements of another component. They can also be used to adapt the mode width to the spot size of a lensed or cleaved

Problem: If we increase the taper angle the insertion loss will converge to the loss of an abrupt junction, which is a taper with 90° taper angle. Estimate the loss of an abrupt 1:2 junction for the standard shallow waveguide structure.

Solution: For the standard shallow waveguide with $N_1 = 3.27$, $N_2 = 3.20$ and $w = 2\ \mu\text{m}$, we find a lateral V-parameter (see eq. 2.78) $V \approx 5.5$, and $V \approx 11$ for the $4\ \mu\text{m}$ wide waveguide. Using Eq. 2.29 we find for the effective mode width $w_e \approx 1.4\ \mu\text{m}$ and $w_e \approx 2.4\ \mu\text{m}$ for 2 and $4\ \mu\text{m}$ waveguide width, respectively. The corresponding Gaussian beamwidths (Eq. 2.30) are $w_1 \approx 1.1\ \mu\text{m}$ and $w_2 \approx 1.9\ \mu\text{m}$, so the width difference is approximately 70% and the loss predicted by Eq. 2.120 is $L \approx 0.6$ dB. Although the match with a 2-dimensional calculation (see Figure 21.5) is not perfect, we see that a simple 1-dimensional analysis gives a fair estimate for the junction loss.

Problem: Do the same for the standard deep-etched waveguide.

Solution: For the standard deep waveguide width $N_1 = 3.27$, $N_2 = 1.0$ and $w = 1.5\ \mu\text{m}$, we find a lateral V-parameter $V \approx 19$, and $V \approx 38$ for the $3\ \mu\text{m}$ wide waveguide. For the effective Gaussian beam widths we find $w_1 \approx 0.66\ \mu\text{m}$ and $w_2 \approx 1.26\ \mu\text{m}$, so the width difference is approximately 90% and the loss predicted by Eq. 2.120 is $L \approx 0.8$ dB. From Figure 21.5 we see that for the deep etched waveguide the deviation of this estimate is a bit larger (1.1 dB), but as a coarse guess it is still reasonable.

Problem 21.3: Insertion loss at an abrupt change in width.

fibre, but only in the lateral direction. For adapting the spot size in two dimensions we need to adapt the vertical dimensions of the waveguide, which is not trivial in a planar integration process.

*fibre-matched
waveguide*

In the JePPIX foundry platforms the problem is solved by integrating a fibre-matched waveguide (FMW) below the normal waveguide, as indicated in Figure 21.6(a). The FMW is created by inserting a few thin quaternary layers in a thick substrate layer below the quaternary waveguide. With the thickness and the position of the thin layers the mode profile can be matched to the vertical mode profile of the fibre, which may be a lensed or High-Contrast Fibre (spot size $3.5\text{-}4\ \mu\text{m}$) or a cleaved fibre ($8\ \mu\text{m}$). For low loss the doping level of the FMW should be low. This approach is, therefore, most suitable for Semi-Insulating Substrates, with a thin n-doped layer directly underneath the quaternary waveguide for serving as n-contact in active components, like SOAs, detectors and modulators. Because this n-doped layer is overlapping only with a small part of the optical flux in the FMW, its contribution to the insertion loss of the FMW can be kept small. Because of the low contrast of the FMW all the light is confined in the quaternary waveguide on top, of which the properties are hardly affected. Their design and operation is in good approximation equal to that of a waveguide without FMW underneath.

The operation of the Spot-Size converter is based on adiabatic conversion of the fundamental modes (both TE and TM) in the quaternary waveguide to the FMW under it. This can be done by gradually tapering the quaternary waveguide to zero and thus forcing the mode to transfer to the lower FMW, as shown in Figure 21.6(b). The tapering can be done in the vertical and the lateral direction. Fraunhofer HHI uses the vertical tapering, as shown in Figure (c), SMART Photonics uses the lateral tapering as

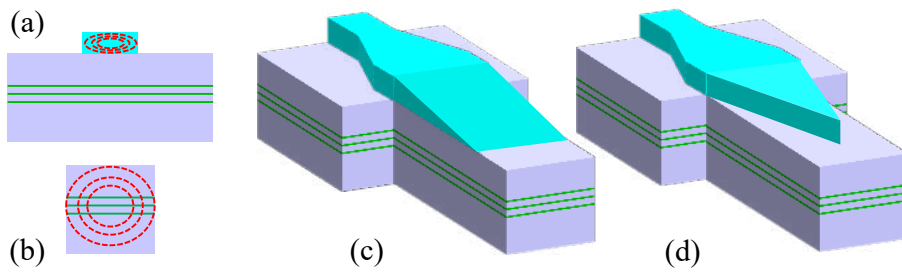


Figure 21.6: (a) standard waveguide on top of an FMW. (b) FMW with the standard waveguide removed. Two-dimensional Spot-Size Converters with vertical tapering (c) and lateral tapering (d).

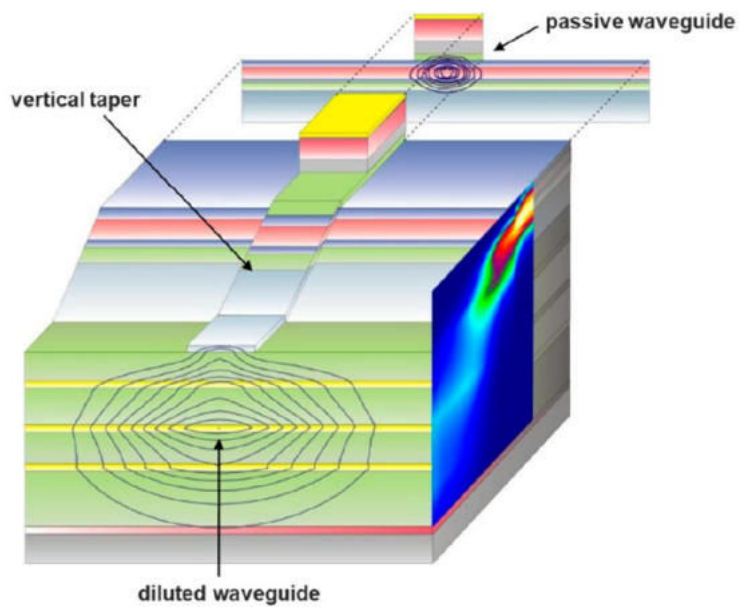


Figure 21.7: 3D-view of the Spot-Size Converter of HHI

shown in Figure (d). For the vertical tapering a non-planar etching process is required in order to achieve a gradual increase in etch-depth along the taper. This requires additional and well-controlled process steps. In a process with shallow and deep etched waveguides the lateral tapering does not require additional process steps, in principle, but it requires a very high resolution of the lithography, because the transfer of the mode to the lower FMW occurs in the region where the taper width decreases from 0.5 to 0.1 μm . So the taper tip has to be very sharp, down to 100 nm, which requires DUV-lithography or Electron-Beam lithography. The latter is not convenient for mass production. In order to reduce the total length of the SSC it is recommended to taper the first part of the waveguide fast and the last part, where the conversion to the FMW takes place, much slower.

The design of the SSC with vertical tapering as shown in Figure 21.6(c) can be done by applying a 2d beam-BPM or FDTD method in the vertical direction, although for accurate design a 3d-method is recommended. For the SSC with lateral tapering as shown in Figure (d) a 3d method is required. If the SSC should be polarisation independent the analysis has to be done for both polarisations and the length has to be chosen for the worst polarisation case. As the taper is adiabatic, this will have little effect for the other polarisation.

The adaption of the lateral spot size is done before the vertical SSC with a waveguide taper as described in the previous section.

21.2.1 Additional information on the HHI SSC

As described above, the HHI SSC is based on the vertical tapered waveguide layer as shown in Figure 21.6c. Three thin Q(1.06) layers running deep below the surface and under all the structures, are used on the spot-size converters (SSCs) to form a so-called diluted waveguide at the facets. Figure 21.7 shows a detailed 3D-schematic of the Spot-Size Converter. The diluted waveguide has a much larger mode size (mode size = 10 x 7 μm^2) than that of the other waveguides, and it allows for an efficient and alignment-tolerant in/out-coupling to a single-mode fiber with less than 2 dB coupling loss. The vertical and horizontal -1 dB alignment tolerance for a wavelength of 1.55 μm is increased from $\pm 0.25 \mu\text{m}$ (lensed fiber) to $\pm 2.5 \mu\text{m}$ (cleaved fiber) and from $\pm 0.5 \mu\text{m}$ to $\pm 3.5 \mu\text{m}$ respectively [283].

21.2.2 Additional information on the SMART Photonics SSC

The SMART Photonics taper is based on a lateral waveguide taper as shown in Figure 21.6d. An advantage of the lateral taper is that it can be formed in the same process steps that are used for defining the shallow and deep etched waveguides. The taper requires a high resolution process because the smooth vertical conversion of the mode requires that the taper width can be smoothly reduced to about 100 nm. With the 193 nm scanner lithography that is used in the foundry process of SMART Photonics, this is possible. Figure 21.8 gives a SEM-photograph of a lateral taper realized in the standard waveguide process. The lateral mode diameter is controlled by the width of the deep etched ridge, the vertical diameter by the thickness of the Fibre-Matched waveguide below the normal waveguide stack. Fibre coupling efficiencies well below 1 dB are feasible with this process.

The integration of the SSC in the standard process affects the process and the performance of the existing building blocks significantly. This is the reason that the process is not yet offered in the standard foundry process. The main additional requirements

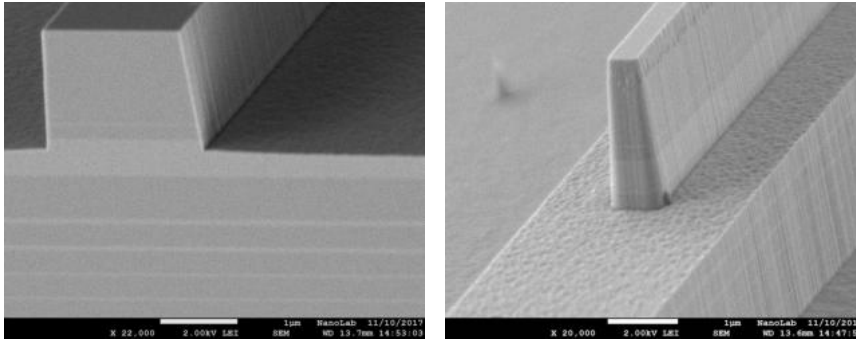


Figure 21.8: SSC in the SMART Photonics platform. Standard waveguide with FMW layers visible below (left) and close-up of the taper tip of the SSC (right)

are a thick epitaxial layer stack below the normal waveguide stack and an additional deep etch step. This makes the process more expensive, which is not yet justified for current applications. For future platforms, an SSC will be introduced.